MiRNAs Expressed at High Levels in Cardiac Muscle are Associated with Insulin and Calcium Signaling Pathways

Ya Tan, Jideng Ma, Yingkai Liu, Keren Long, Liujun He, Xuewei Li and Li Zhu
Institute of Animal Genetics and Breeding, College of Animal Science and Technology,
Sichuan Agricultural University, 625014 Ya'an, China

Abstract: MicroRNAs (miRNAs) are non-coding RNAs that negatively regulate gene expression. Compelling evidences have demonstrated the important roles of miRNAs in muscle proliferation, differentiation and development processes. Cardiac muscle and skeletal muscle (longissimus dorsi muscle and psoas major muscle) are both striated muscles which perform different functions *in vivo*. However, little is known about the differences of miRNA expression pattern between these distinct muscles. In this study, researchers applied a deep sequencing approach to identify the miRNA transcriptomes between cardiac and skeletal muscles. Three sequencing libraries were constructed from three 210 days old pigs, a total of 56 M raw data was generated with 95.58% of them were mappable sequences. In total, 321 unique miRNAs were identified in three sequencing libraries of which 109 were differentially expressed. Ranking analysis showed that six out of the ten most highly expressed miRNAs in cardiac muscle were up-regulated compared with longissimus dorsi muscle and psoas major muscle. GO and KEGG pathway analyses for the predicted target genes of the six up-regulated miRNAs showed that the miRNAs highly expressed in CM are mainly involved in insulin and calcium signaling pathways and the constructed miRNA-mRNA interaction networks highlighted the important differences between cardiac and skeletal muscles, all these results may promote the researches on muscle-related diseases in a certain degree.

Key words: miRNA, cardiac muscle, skeletal muscle, deep sequencing, pig

INTRODUCTION

Cardiac muscle and skeletal muscle are two different types of striated muscle that derived from embryonic mesoderm in vertebrates. Cardiomyocytes also called myocardiocytes, the major cell type of cardiac muscle, mainly contain two nuclei and are branched. While skeletal muscle cells are called myofibers and have multicellular syncytia both linear and longitudinal. These cells form the different structures and may underlie differences in functional characteristics between cardiac and skeletal muscles.

MicroRNAs (miRNAs) are a family of non-coding RNAs, approximately 22 nucleotides (nt) in length which inhibit the expression of target genes through translational repression or mRNA degradation via base-pairing with mRNA transcripts (Lee *et al.*, 1993; Wightman *et al.*, 1993). The involvement of miRNAs in multiple physiological and pathological processes had been demonstrated by numerous studies. MiR-1 and miR-133 are the best-characterized muscle-specific miRNAs. MiR-1 can induce the differentiation of

mesodermal and muscle lineages and the function of miR-133a is to regulate proliferation and differentiation in a cell type and signal-specific manner. They both play important roles in the proliferation and differentiation of skeletal muscle as well as in cardiac growth, differentiation and conductance and are involved in cardiogenesis, myogenesis and muscle hypertrophy (McCarthy and Esser, 2007). In addition, abnormal expression of miRNAs can cause muscle dysfunction and disease such as muscular dystrophy (McCarthy *et al.*, 2007), arrhythmias (Yang *et al.*, 2007) and myocardial infarction (Van Rooij *et al.*, 2008).

The previous study revealed metabolic differences between Longissimus Dorsi Muscle (LDM) and Psoas Major Muscle (PMM) (Liu *et al.*, 2013) which are representative of the two major muscle types in skeletal muscle but the relationships and differences of miRNA expression between skeletal and cardiac muscles are poorly understood. Here, researchers describe a comprehensive analysis to identify the differences of miRNA transcriptomes between cardiac and skeletal muscles by deep sequencing approach. Several

---

Corresponding Author: Li Zhu, Institute of Animal Genetics and Breeding, College of Animal Science and Technology,
Sichuan Agricultural University, 625014 Ya'an, China

miRNAs were identified to reveal the differential expression pattern. Furthermore, researchers also analyzed the target genes of differentially expressed miRNAs and constructed dynamic networks of insulin and calcium signaling pathways during heart development based on miRNA-mRNA interactions to understand the potential biological functions.

MATERIALS AND METHODS

Ethics statement: All studies involving animals were conducted according to the Regulations for the Administration of Affairs Concerning Experimental Animals (Ministry of Science and Technology, China, revised in June 2004) and approved by the Institutional Animal Care and Use Committee in the College of Animal Science and Technology, Sichuan Agricultural University, Sichuan, China under permit No. DKY-S20112744. Animals were allowed access to feed and water *ad libitum* under the same normal conditions and were humanely sacrificed as necessary to ameliorate suffering.

RNA extraction: The Cardiac Muscle (CM), Longissimus Dorsi Muscle (LDM) and Psoas Majormuscle (PMM) of three female Landrace pigs (210 days old) were dissected, quickly frozen in liquid nitrogen and then stored at -80°C. Small RNA was separately isolated and purified by using mirVana™ miRNA Detection kit (Ambion, Austin, TX, USA) according to the manufacturer's procedure. The quality and purity of total RNA were assessed using a NanoDrop ND-1000 spectrophotometer (NanoDrop, Wilmington, DE, USA) at 260/280 nm (ratio >2.0). The integrity of total RNA was also monitored via analysis by the Bioanalyzer 2100 and RNA 6000 Nano LabChip kit (Agilent, CA, USA) with RIN number >6.0. All results illustrated that RNA was high purity as well as integrity and could be used for deep sequencing.

Library construction and deep sequencing: For a certain muscle tissue, equal amounts (5 μg) of small-RNA-enriched total RNA isolated from three female pigs were pooled and used for library preparation and deep sequencing. Each sample was size-fractionated by Polyacrylamide Gel Electrophoresis (PAGE) and RNA fragments of 10-40 nt (nucleotide) length were collected then followed by 3' and 5' adaptors ligation (Illumina, San Diego, CA, USA) and PCR. The small RNA fractions were then converted to cDNA by RT-PCR and the amplification products were purified using PAGE. The purified three libraries were directly used for cluster generation with Illumina's Cluster Station and then sequenced on the Genome Analyzer GA-II X (Illumina) according to the manufacturer's protocol.

In silico analysis of deep sequenced small RNA: The sequenced sequences were analyzed using a proprietary pipeline, ACGT101-miR program (Illumina) and followed a series of additional filters (Li *et al.*, 2011, 2010a, b). The resulting sequences are referred to as mappable sequences. The mappable sequences were then mapped to the pig genome (~2.26 Gb, Sscrofa9) using the NCBI local BLAST package (http://blast.ncbi.nlm.nih.gov/), the mapping progress are as follows: map the mappable sequences to the 271 known porcine pre-miRNAs (encoding 306 miRNAs) in miRBase 19.0 (August 2012); map the mappable sequences to the pig genome to obtain their genomic locations and the corresponding annotations from Ensembl release 73 (Sscrofa 10.2, August 2011).

Differentially expressed miRNAs and KEGG analysis: To determine the significant differences of miRNA counts in each library, the IDEG6 Program (Romualdi *et al.*, 2003) was used for the normalized calculation among the mappable sequences in the three libraries. Three statistics tests (Audic and Claverie test, Fisher exact test and χ^2-test) were applied in the significance test and differentially expressed miRNAs were picked up when three tests produced $p<10^{-6}$ simultaneously by pairwise comparison among three libraries. The pairwise overlaps of PicTar (Krek *et al.*, 2005) and TargetScan (Lewis *et al.*, 2003, 2005) were used to predict the target mRNA of miRNAs and then *DAVID* (Huang *et al.*, 2008a) gene annotation analysis was used to analyze the possible biological functions of target mRNAs. Only GO terms and KEGG pathways with p<0.01 were chosen.

Quantitative real-time PCR (qPCR): Fourteen miRNAs were selected to validate and characterize the expression identified by deep sequencing. Their relative expression levels were analyzed at four developmental stages (0, 30, 210 days and 7 years) in these three muscle tissues from three female Landrace pigs by real-time PCR approach. The forward primer of miRNA was identical in sequences and lengths to the miRNA itself (i.e., the most abundant isomiR) based on the sequencing results. Several mRNAs involved in insulin signaling and calcium signaling pathways were also selected in this analysis and the primers were in Table 1. Quantitative real-time PCR analysis for miRNAs and mRNAs were performed with the

Table 1: Pearson's correlation analysis between deep sequencing and qRT-PCR

miRNAs	Experimental approach	Pearson's correlation	p-values
miR-378	Sequencing qRT-PCR	0.94	0.11
miR-499	Sequencing qRT-PCR	0.99	0.03
miR-206	Sequencing qRT-PCR	0.99	0.02
miR-208b	Sequencing qRT-PCR	0.98	0.04
miR-139	Sequencing qRT-PCR	0.99	0.04

SYBR®PrimeScript™ miRNA RT-PCR kit (TaKaRa Bio Inc., China) and SYBR® Premix Ex Taq™ II (TaKaRa Bio Inc., China), respectively on the CFX96™ Real-Time PCR Detection System (Bio-Rad, CA, USA). All reactions were run in triplicate. The relative expression quantification was calculated using the $2^{-\Delta\Delta Ct}$ Method and was normalized with the internal control genes (miRNA: U6 snRNA, 5S rRNA, 18S rRNA; mRNA: YWHAC, RLP4, PPIL). The each miRNA expression level was presented as means±SD (standard deviation) and error bars indicated the standard deviation.

RESULTS AND DISCUSSION

Overview of deep sequencing data: A total of 56 M (Million) raw reads were generated from three libraries using Illumina's sequencing platform. After applying a series of filter criteria, the accepted sequences were considered as mappable sequences (see methods) and researchers acquired 20.31 M (94.12%), 15.87 M (95.48%) and 17.93 M (97.14%) mappable sequences in CM, LDM and PMM libraries, respectively. To make the sequencing data more reliable, the low-abundance mappable sequences (reads <3) were eliminated.

The length distribution of mappable sequences in the three libraries was similar (Fig. 1). The vast majority of mappable sequences were 21-23 nt in length (95.29±0.80%, n = 3), more than half of them were 22 nt in length (88.52±4.15%, n = 3), the next most abundant were 21 nt (4.52±2.36%, n = 3) and 23 nt (2.24±1.03%, n = 3) these were consistent with the typical size range for Dicer-derived products (Blaszczyk *et al.*, 2001).

Differentially expressed miRNAs: According to the sequencing results, 321 mature miRNAs corresponding to
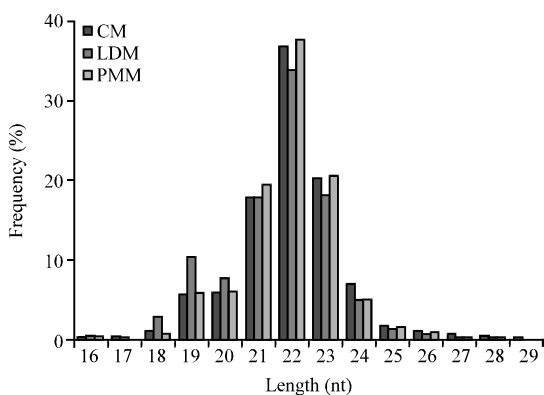

Fig. 1: Length distribution of miRNAs in three libraries. The y-axis indicates the ratio of miRNAs (numbers of each stage divided by total numbers in a library)

271 known porcine pre-miRNAs were identified in the study. These known porcine miRNAs accounted for the vast majority of the total reads in each library (99.39, 96.45 and 97.19% for CM, LDM and PMM, respectively). To date, miRBase 19.0 (August 2012) has documented 271 pre-miRNAs encoding 306 known porcine miRNAs. The high coverage of known porcine miRNAs illustrates that the small RNA sequencing and miRNA-identification pipeline are of high confidence.

Of the 321 identified miRNAs, 109 were found to be differentially expressed among the three libraries. Four differentially expressed miRNAs were randomly selected for qPCR validation and the correlation analysis showed that there was a significantly positive correlation between qPCR and deep sequencing results (average Pearson's r = 0.98, p<0.01) (Table 2) which also highlight the reliability of the sequencing data. Based on the expression levels of 109 differentially expressed miRNAs, hierarchical clustering analysis (Fig. 2a) and correlation analysis (Fig. 2b) were performed to reveal miRNA expression differences among the three muscle tissues. As shown in Fig. 2, LDM and PMM had a more similar expression pattern (Pearson's r = 0.94, p<0.01) compared with those between LDM and CM (Pearson's r = 0.79, p<0.01) and between PMM and CM (Pearson's r = 0.82, p<0.01) indicating a closer relationship between the two skeletal muscle types even though some studies had reported that PMM and LDM muscles are distinct muscle fibers with different metabolic features (Li *et al.*, 2010a, b; Liu *et al.*, 2013). The results indicate that skeletal muscle (LDM and PMM) and cardiac muscle are indeed two tissues.

miRNAs with high abundance in CM reveal the differences between two muscle types: Known porcine miRNAs were expressed at considerably different levels, ranging from three to millions of reads however, only a few miRNAs were expressed at the highest levels. In CM, the top ten expressed miRNAs accounted for 82.24% of the unique reads (Fig. 3a). Of these ten miRNAs, eight were differentially expressed and six miRNAs (miR-143, -378, -27b, -30e, -101 and let-7a) were up-regulated (>1.5 fold change) in CM compared to LDM and PMM simultaneously, the qPCR results also confirmed that these miRNAs were up-regulated in CM (average r = 0.97, p<0.01) (Fig. 3b). The most abundant miRNA in CM was miR-143 which is a cardiovascular-specific miRNA and plays key roles in modulating vascular smooth muscle cell phenotypes (Cordes *et al.*, 2009). MiR-378 had a high expression level in both cardiac and skeletal muscle and it is up-regulated during muscle differentiation by increasing MyoD

Table 2: Enriched GO terms for target genes of CM up-regulated miRNAs

Categories	GO ID	Description	Involved gene count	p-values
GO-BP	GO:0001568	Blood vessel development	33	2.59×10^{-4}
GO-BP	GO:0007507	Heart development	32	5.13×10^{-5}
GO-BP	GO:0048514	Blood vessel morphogenesis	26	4.45×10^{-9}
GO-BP	GO:0007517	Muscle organ development	26	4.45×10^{-9}
KEGG-PATHWAY	hsa04020	Calcium signaling pathway[1]	25	1.44×10^{-9}
GO-BP	GO:0042692	Muscle cell differentiation	22	5.72×10^{-5}
KEGG-PATHWAY	hsa04910	Insulin signaling pathway[2]	21	1.28×10^{-9}
GO-BP	GO:0060537	Muscle tissue development	19	1.86×10^{-8}
GO-BP	GO:0032868	Response to insulin stimulus[2]	18	3.65×10^{-4}
KEGG-PATHWAY	hsa05414	Dilated cardiomyopathy	16	1.95×10^{-9}
GO-BP	GO:0032869	Cellular response to insulin stimulus[2]	14	5.55×10^{-4}
KEGG-PATHWAY	hsa05410	Hypertrophic Cardiomyopathy (HCM)	14	6.70×10^{-9}
KEGG-PATHWAY	hsa04930	Type II diabetes mellitus[2]	13	7.74×10^{-5}
GO-BP	GO:0008016	Regulation of heart contraction	12	1.41×10^{-9}
GO-BP	GO:0051592	Response to calcium ion[1]	9	3.07×10^{-9}
GO-BP	GO:0008286	Insulin receptor signaling pathway[2]	7	3.64×10^{-9}
GO-BP	GO:0046626	Regulation of insulin receptor signaling pathway[2]	5	3.58×10^{-9}
GO-BP	GO:0051926	Negative regulation of calcium ion transport[1]	4	4.29×10^{-9}
GO-MF	GO:0005159	Insulin-like growth factor receptor binding[2]	4	4.36×10^{-9}

[1]Description marked is calcium signaling pathway involving GO terms and [2]represent insulin signaling pathway-related GO terms; GO: Gene Ontology; BP: Biological Process; MF: Molecular Function
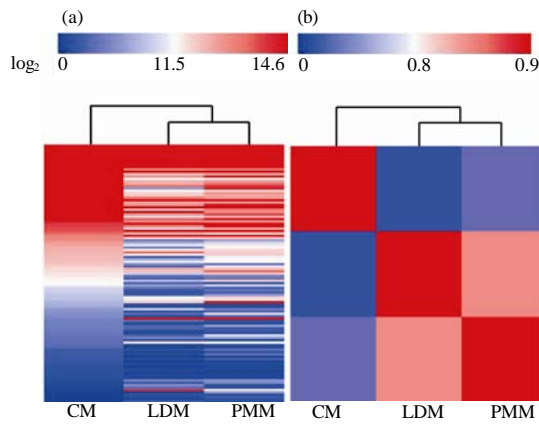

Fig. 2: Heat map matrix of differentially expressed miRNAs among the three libraries; a) Hierarchical clustering analysis based on 109 differentially expressed miRNAs, the data were calculated as $\log_2$; b) Pearson's correlations analysis based on 109 differentially expressed miRNAs

transcriptional activity (Gagan *et al.*, 2011). Let-7a was expressed ubiquitously in all three libraries and accounted for over 3.03% of the total unique reads. The functions of the other high-abundance miRNAs (miR-27b, -30e and -101) have not been documented yet. Subsequently, researchers selected these six most up-regulated miRNAs to further analyze their possible biological functions.

These highly expressed miRNAs in CM may reflect biological differences among these distinct muscle types therefore, *in silico* analysis was used to predict their possible roles in muscle development. As a result, a total of 1,366 target genes were predicted and subjected to *DAVID* gene annotation analysis. One hundred and sixty nine GO terms were significantly enriched including muscle organ development, heart development, blood vessel morphogenesis, etc. It was not surprising that the target genes of CM up-regulated miRNAs were enriched in heart-related diseases such as dilated cardiomyopathy and Hypertrophic Cardiomyopathy (HCM). Intriguingly, researchers also found the enrichment of several GO terms for gene annotation analysis such as response to insulin stimulus, insulin-like growth factor receptor binding and negative regulation of calcium ion transport. These terms are related to insulin and calcium signaling pathways and describe vital roles in muscle metabolism, muscle contraction and cardiac hypertrophy (Table 3).

Insulin and calcium signaling pathways regulated by miRNA-mRNA interactions: In order to further illustrate the role of miRNAs in CM-specific features with respect to insulin and calcium signaling networks, several experimentally validated miRNA-mRNA pairs that are involved in insulin and calcium signaling pathways were selected. To verify the negatively correlated relationship of these miRNA-mRNA pairs, researchers detected the expression levels of these miRNAs and mRNAs in CM during four muscle developmental stages (including 0, 30, 210 days and 7 years) and then constructed regulatory networks based on miRNA-mRNA interactions involved in insulin and calcium signaling pathways (Fig. 4 and 5).

Akt (also known as protein kinase B, PKB), IRS1 (Insulin Receptor Substrate 1), IGF1R (insulin receptor 1), FOXO1 (Forkhead box O1) and PI3K (Phosphoionositide-3-Kinase) are key factors in the insulin signaling pathway that participate in the regulation of glucose and lipid
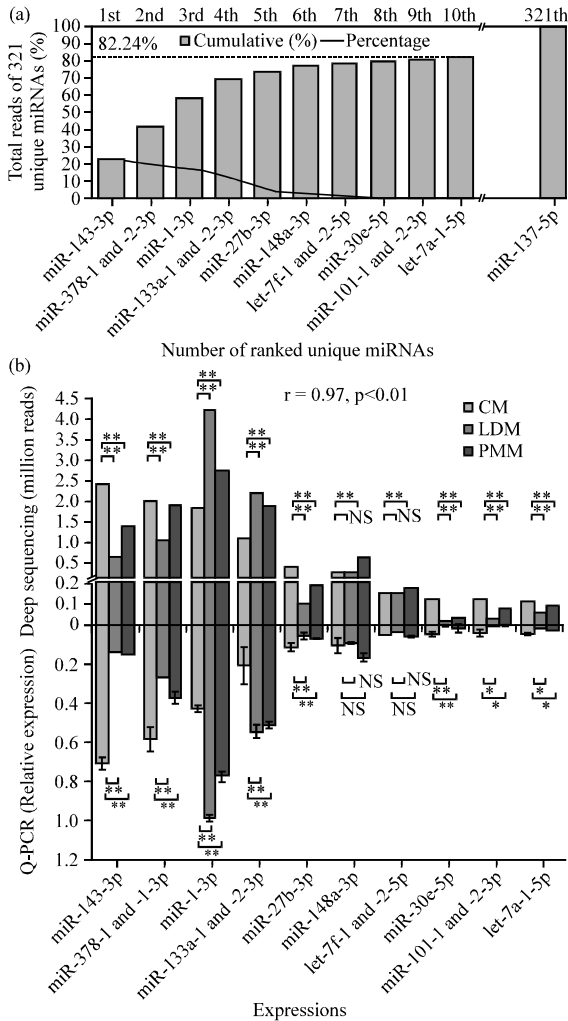
Fig. 3: Expression characteristics of the most highly expressed miRNAs in the three libraries; a) The ten most highly expressed unique miRNAs in CM. The unique miRNAs (starting from the miRNA with the highest number of reads, x-axis) versus their cumulative % of the total counts from 321 unique miRNAs detected in the three libraries are shown. The dashed line at 82.24% represents the cumulative level of the ten most highly expressed unique miRNAs in CM. The gray line indicates the expression % of individual miRNAs; b) The top ten expressed miRNAs in CM across the three sequencing libraries and qPCR results. The IDEG6 program was used for normalization calculation in three libraries and the one-way ANOVA analysis was applied to qPCR results. All ten miRNAs showed differential expression between CM and PMM and eight miRNAs showed differential expression between CM and LDM (**p<0.01; *p<0.05; NS: No Significance)

homeostasis, anti-apoptosis, proliferation and differentiation. The qPCR results (Fig. 4) showed that miR-145, -378 and -29 negatively regulate their target genes *IRS1*, *IGF1R* and *PI3K*, respectively. Pandey *et al.* (2011) reported that miR-29a targets the p85α subunit of PI3K and abrogates downstream insulin signaling in HepG2 cells (Pandey *et al.*, 2011). Meanwhile, miR-29a has a negative effect on insulin signaling by indirect inhibition of Akt (He *et al.*, 2007). The deep sequencing data revealed a lower abundance of miR-29a in CM compared to that in skeletal muscle (1.36 fold change) which might lead to relatively higher expression of PI3K and Akt in CM. The imbalance between fatty acid uptake and β-oxidation may contribute to muscle insulin resistance. It should be noted that heart and skeletal muscle could have very different metabolic rates upon fatty acid oxidation. Heart muscle is highly oxidative while skeletal muscles consist of different fiber types and only slow-twitch fibers (e.g., PMM) have a high oxidative capacity (Bottinelli and Reggiani, 2000; Essen *et al.*, 1975). Nevertheless, 70% of whole body glucose disposal occurs in skeletal muscle (DeFronzo *et al.*, 1981) and about 90% of fatty acid β-oxidation is for energy demand (Kelley *et al.*, 1993). Therefore, any perturbation of insulin sensitivity in skeletal muscle may provoke metabolic abnormality at the level of the whole body. A large number of factors maintain normal heart function and the regulatory mechanisms involved are complicated. The conversion and accumulation of any lipid intermediates has been implicated not only in the development of insulin resistance but also in cardiac dysfunction and heart failure (Muoio and Newgard, 2008; Summers, 2006) making insulin resistance in cardiac muscle more complex to research.

CACN1C (calcium channel, voltage-dependent, L type, alpha 1C subunit), ATP2B2 (ATPase, Ca^{++} transporting, plasma membrane 2), CaM (calmodulin), CaN (calcineurin) and CAMK (calcium/calmodulin-dependent protein kinase II delta) play important roles in calcium signaling and they are highly involved in muscle contraction and metabolism as well as proliferation and other signaling pathways. As shown in Fig. 5, six out of seven miRNA-mRNA pairs were inversely correlated with each other, suggesting that these miRNAs participate in calcium signaling by inhibiting their bona fide target mRNAs during muscle development. Both miR-1 and -133a were up-regulated (by 1.86 fold and 1.79 fold, respectively) in skeletal muscle, suggesting lower CaM and CaN expression levels in skeletal muscle. It is well established that muscle hypertrophy is a calcium-dependent process and that elevations in

Table 3: Primers in quantitative real-time PCR

Genes	Gene accession	Sequence of primers	Length of products (bp)
CALM1	NM_001244210	F: GCACCATCACAACAAAGGAAC	111
		R: TGCCATTACCATCAGCGTC	
CaN	NM_001243913	F: CACAGATGGGAATGGAGAAG	108
		R: TAGATACGGAAAGCAAACCT	
CAMK2D	NM_214381	F: CAAGCGTATCACAGCCTCAG	142
		R: CAAGATGGCACCCTTTAGTTT	
PIK3R5	NM_213851	F: ACAGACCCCTAAATCCAAGAAG	155
		R: CCTCGCACCTGATGACACTC	
Cav1	NM_214438	F: CCCAAGCATCTCAACGACGAC	152
		R: AGGGCAGACAGCAAACGGT	
CACNA1C	XM_005664126	F: GCTTCGCCGTCTTCTATTTCA	177
		R: TGGCTTCAGGGTCATACTCC	
ATP2B2	XM_005674148	F: CCTTTTCATCCAGGGCAAT	139
		R: CACCATCCGTCCAGAACCCT	
IRS1	NM_001244489	F: ACCTGATTGGCATCTACC	235
		R: CCTCCAGGATTGTCTCAT	
IGF1R	NM_214172	F: TGGATGCCGTGTCCAAT	256
		R: GTGTCGTTGTCGGGTGC	
Akt1	NM_001159776	F: AAGACCTTCTGTGGGACG	315
		R: GATGCTGGCGAAGAAACG	
FOXO1	NM_214014	F: GTCTGCCGTCAATGGG	101
		R: GCACTTGTAAAGCGGTCTT	
MURF1	NM_001184756	F: GTGACAAAGGCAAGACCC	195
		R: ACACGGCAAGATGACCACC	
*YWHAZ**	DQ178130	F: ATTGGGTCTGGCCCTTAACT	146
		R: GCGTGCTGTCTTTGTATGACTC	
*PPIA**	NM_214353	F: CACAAACGGTTCCCAGTTTT	171
		R: TGTCCACAGTCAGCAATGGT	
*RPL4**	DQ845176	F: AGGAGGCTGTTCTGCTTCTG	185
		R: TCCAGGGATGTTTCTGAAGG	

YWHAZ (Tyrosine 3-monooxygenase/tryptophan 5-monooxygenase activation protein, zeta polypeptide), *PPLA* (P-Phenethyl L-Aspartate), *RPL4* (Ribosomal Protein L4) are the internal control genes
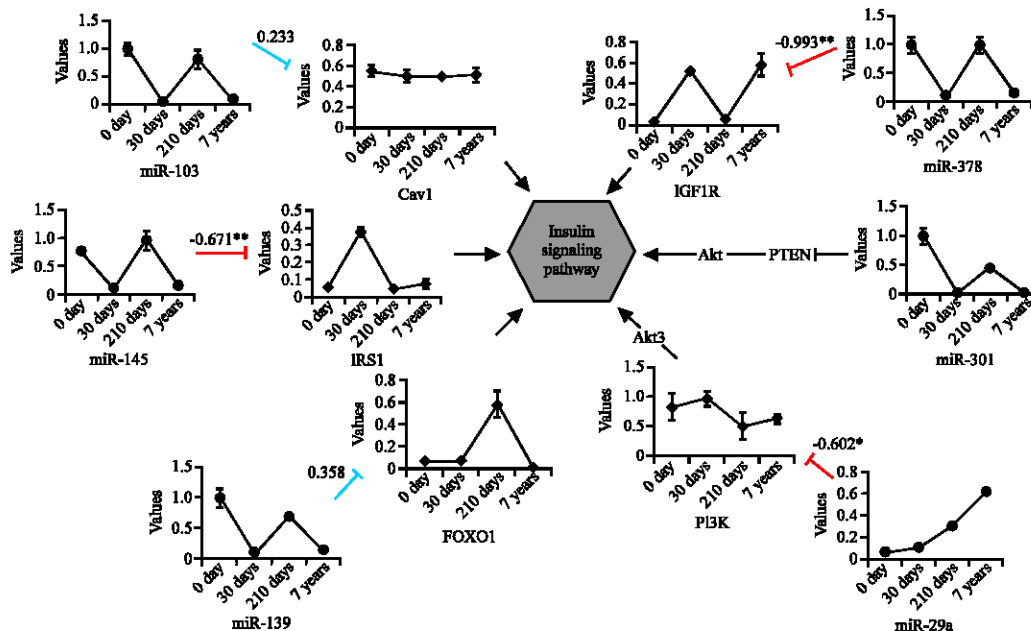

Fig. 4: The network of miRNAs and mRNAs involved in the insulin signaling pathway. A Pearson's correlation was calculated between each pair of miRNA-mRNAs. The graphs indicate the expression level of miRNAs or mRNAs (y-axis) with respect to muscle development (x-axis) and the blue and red connecting lines show positive and negative correlations (*p<0.05, **p<0.01), respectively. Cav1: Caveolin 1; IRS1: Insulin Receptor Substrate 1; FOXO1: Forkhead box O1; PI3K: Phosphoinositide-3-Kinase; PTEN: Phosphatase and Tensin homolog deleted on chromosome ten; IGF1R: Insulin Receptor 1; Akt: Also known as Protein Kinase B (PKB)
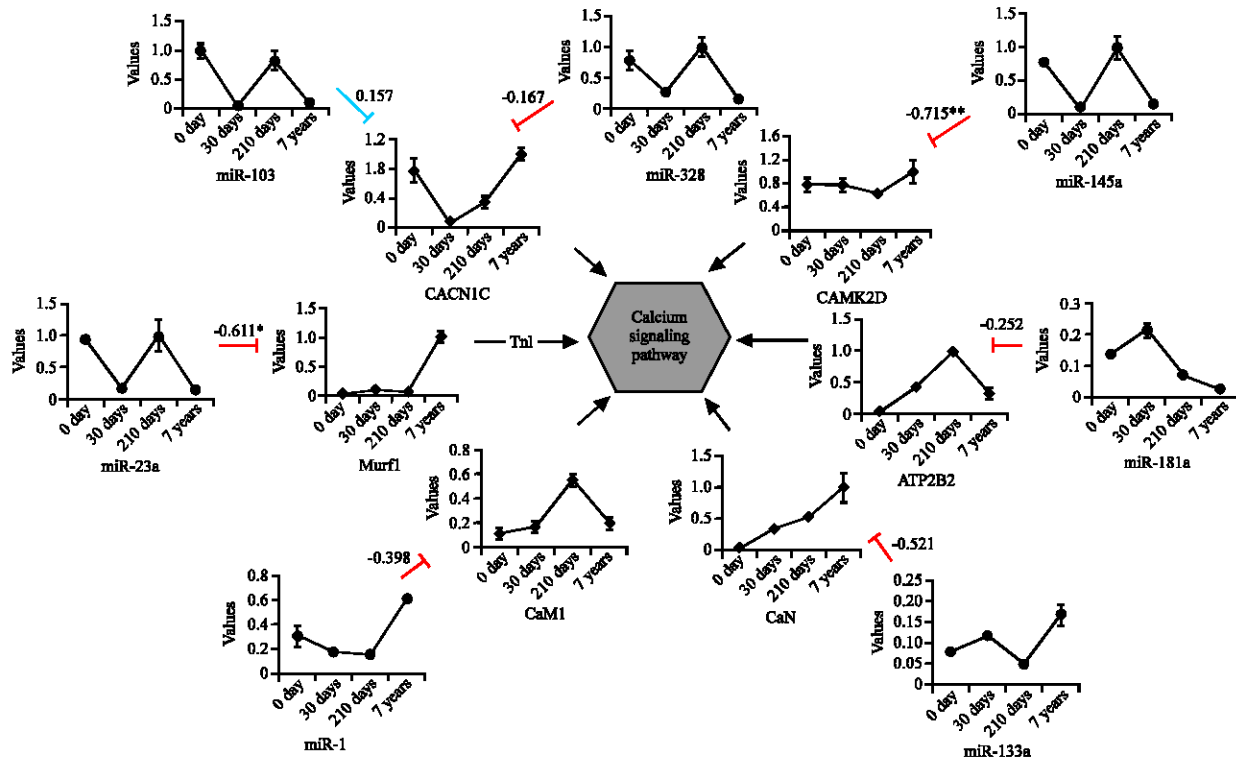
Fig. 5: The network of miRNAs and mRNAs involved in the calcium signaling pathway. A Pearson's correlation was calculated between each pair of miRNA-mRNAs. The graphs indicate the expression level of miRNAs or mRNAs (y-axis) with respect to muscle development (x-axis) and the blue and red connecting lines show positive and negative correlations (*p<0.05, **p<0.01), respectively. CACN1C: Calcium Channel, voltage-dependent, L type, alpha 1C subunit; Murf1: Muscle ring finger 1; CaM1: Calmodulin 1; CaN: Calcineurin; ATP2B2: ATPase, Ca^{++} transporting, plasma membrane 2; CAMK2D: Calcium/Calmodulin-dependent protein Kinase 2 Delta

intracellular calcium levels are essential for muscle contraction via the actin thin filament-associated troponin-tropomyosin system (Gordon *et al.*, 2000; Leavis *et al.*, 1984; Tobacman, 1996). TnT (TroponinT) is the tropomyosin-binding subunit of the troponin complex (Perry, 1998) and plays a coordinator role in the Ca^{2+} regulatory system of muscles. A major difference between cardiac and skeletal muscles is their TnT isoform contents. In contrast to skeletal muscle which simultaneously expresses multiple TnT isoforms, normal adult human cardiac muscle contains a single isoform of cardiac TnT. This is to guarantee the ventricular myocardium functions as an electrophysiological syncytium, accomplishing the synchronized contraction that is critical to the rhythmic pumping function of the vertebrate heart (Huang *et al.*, 2008b). Taken together, researchers tentatively conclude that the processes of cardiac muscle and skeletal muscle development are regulated by differential expression of miRNAs and their target genes which are involved in insulin and calcium signaling pathways.

CONCLUSION

Researchers have identified important differences in miRNA expression patterns in porcine cardiac and skeletal muscles which are mainly related to insulin and calcium signaling pathways. The results provide crucial information that increases the understanding of porcine cardiac and skeletal muscles. In addition, the study may provide a theoretical basis for the diagnosis and therapy of muscle-related diseases.

ACKNOWLEDGEMENTS

REFERENCES

Blaszczyk, J., J.E. Tropea, M. Bubunenko, K.M. Routzahn, D.S. Waugh and X. Ji, 2001. Crystallographic and modeling studies of RNase III suggest a mechanism for double-stranded RNA cleavage. Structure, 9: 1225-1236.

Bottinelli, R. and C. Reggiani, 2000. Human skeletal muscle fibres: Molecular and functional diversity. Prog. Biophys. Mol. Biol., 73: 195-262.

Cordes, K.R., N.T. Sheehy, M.P. White, E.C. Berry and S.U. Morton *et al.*, 2009. miR-145 and miR-143 regulate smooth muscle cell fate and plasticity. Nature, 460: 705-710.

DeFronzo, R.A., E. Jacot, E. Jequier, E. Maeder, J. Wahren and J.P. Felber, 1981. The effect of insulin on the disposal of intravenous glucose: Results from indirect calorimetry and hepatic and femoral venous catheterization. Diabetes, 30: 1000-1007.

Essen, B., E. Jansson, J. Henriksson, A. Taylor and B. Saltin, 1975. Metabolic characteristics of fibre types in human skeletal muscle. Acta Physiol. Scand., 95: 153-165.

Gagan, J., B.K. Dey, R. Layer, Z. Yan and A. Dutta, 2011. MicroRNA-378 targets the myogenic repressor MyoR during myoblast differentiation. J. Biol. Chem., 286: 19431-19438.

Gordon, A.M., E. Homsher and M. Regnier, 2000. Regulation of contraction in striated muscle. Physiol. Rev., 80: 853-924.

He, A., L. Zhu, N. Gupta, Y. Chang and F. Fang, 2007. Overexpression of micro ribonucleic acid 29, highly up-regulated in diabetic rats, leads to insulin resistance in 3T3-L1 adipocytes. Mol. Endocrinol., 21: 2785-2794.

Huang, D.W., B.T. Sherman and R.A. Lempicki, 2008a. Systematic and integrative analysis of large gene lists using DAVID bioinformatics resources. Nat. Protocols, 4: 44-57.

Huang, Q.Q., H.Z. Feng, J. Liu, J. Du and L.B. Stull *et al.*, 2008b. Co-expression of skeletal and cardiac troponin T decreases mouse cardiac function. Am. J. Physiol. Cell Physiol., 294: C213-C222.

Kelley, D.E., M. Mokan, J.A. Simoneau and L. Mandarino, 1993. Interaction between glucose and free fatty acid metabolism in human skeletal muscle. J. Clin. Invest., 92: 91-98.

Krek, A., D. Grun, M.N. Poy, R. Wolf and L. Rosenberg *et al.*, 2005. Combinatorial microRNA target predictions. Nat. Genet., 37: 495-500.

Leavis, P.C., J. Gergely and A.G. Szent-Gyorgyi, 1984. Thin filament proteins and thin filament-linked regulation of vertebrate muscle contractio. Crit. Rev. Biochem. Mol. Biol., 16: 235-305.

Lee, R.C., R.L. Feinbaum and V. Ambros, 1993. The *C. elegans* heterochronic gene lin-4 encodes small RNAs with antisense complementarity to lin-14. Cell, 75: 843-854.

Lewis, B.P., C.B. Burge and D.P. Bartel, 2005. Conserved seed pairing, often flanked by adenosines, indicates that thousands of human genes are microRNA targets. Cell, 120: 15-20.

Lewis, B.P., I.H. Shih, M.W. Jones-Rhoades, D.P. Bartel and C.B. Burge, 2003. Prediction of mammalian microRNA targets. Cell, 115: 787-798.

Li, M., Y. Liu, T. Wang, J. Guan and Z. Luo *et al.*, 2011. Repertoire of porcine MicroRNAs in adult ovary and testis by deep sequencing. Int. J. Biol. Sci., 7: 1045-1055.

Li, M., Y. Xia, Y. Gu, K. Zhang and Q. Lang *et al.*, 2010a. MicroRNAome of porcine pre and postnatal development. PloS ONE, Vol. 5. 10.1371/journal. pone.0011541.

Li, Y., Z. Xu, H. Li, Y. Xiong and B. Zuo, 2010b. Differential transcriptional analysis between red and white skeletal muscle of Chinese Meishan pigs. Int. J. Biol. Sci., 6: 350-360.

Liu, Y., M. Li, J. Ma, J. Zhang and C. Zhou *et al.*, 2013. Identification of differences in microRNA transcriptomes between porcine oxidative and glycolytic skeletal muscles. BMC Mol. Biol., Vol. 14. 10.1186/1471-2199-14-7

McCarthy, J.J. and K.A. Esser, 2007. MicroRNA-1 and microRNA-133a expression are decreased during skeletal muscle hypertrophy. J. Appl. Physiol., 102: 306-313.

McCarthy, J.J., K.A. Esser and F.H. Andrade, 2007. MicroRNA-206 is overexpressed in the diaphragm but not the hindlimb muscle of mdx mouse. Am. J. Physiol. Cell Physiol., 293: C451-C457.

Muoio, D.M. and C.B. Newgard, 2008. Molecular and metabolic mechanisms of insulin resistance and β-cell failure in type 2 diabetes. Nat. Rev. Mol. Cell Biol., 9: 193-205.

Pandey, A.K., G. Verma, S. Vig, S. Srivastava, A.K. Srivastava and M. Datta, 2011. miR-29a levels are elevated in the db/db mice liver and its overexpression leads to attenuation of insulin action on PEPCK gene expression in HepG2 cells. Mol. Cell. Endocrinol., 332: 125-133.

Perry, S., 1998. Troponin T: Genetics, properties and function. J. Muscle Res. Cell. Motil., 19: 575-602.

Romualdi, C., S. Bortoluzzi, F. d'Alessi and G.A. Danieli, 2003. IDEG6: A web tool for detection of differentially expressed genes in multiple tag sampling experiments. Physiol. Genomics, 12: 159-162.

Summers, S.A., 2006. Ceramides in insulin resistance and lipotoxicity. Prog. Lipid Res., 45: 42-72.

Tobacman, L.S., 1996. Thin filament-mediated regulation of cardiac contraction. Annu. Rev. Physiol., 58: 447-481.

Van Rooij, E., L.B. Sutherland, J.E. Thatcher, J.M. DiMaio and R.H. Naseem *et al.*, 2008. Dysregulation of microRNAs after myocardial infarction reveals a role of miR-29 in cardiac fibrosis. Proc. Nat. Acad. Sci. USA., 105: 13027-13032.

Wightman, B., I. Ha and G. Ruvkun, 1993. Posttranscriptional regulation of the heterochronic gene lin-14 by lin-4 mediates temporal pattern formation in *C. elegans.* Cell, 75: 855-862.

Yang, B., H. Lin, J. Xiao, Y. Lu and X. Luo *et al.*, 2007. The muscle-specific microRNA miR-1 regulates cardiac arrhythmogenic potential by targeting GJA1 and KCNJ2. Nature Med., 13: 486-491.